

Using ultrasonography for evaluating normal and some abnormal reproductive systems in straight Egyptian Arabian mares

Haitham A. Barbary

Diagnostic Imaging and Endoscopy Unit, Animal Reproduction Research Institute, Egypt

Abstract

Ultrasound is an important diagnostic method for monitoring the reproductive system of mares. In this research, thirty reproductive straight Egyptian Arabian mares were followed using transrectal ultrasound. Using rectal ultrasonography, the reproductive condition of these mares was diagnosed instantaneously, with mares that suffered from reproductive problems (endometritis and endometrial cysts) and healthy ones that were pregnant and not pregnant. Infectious endometritis and uterine cysts caused abnormal reproductive issues in our work. From the routine use of ultrasonography, we confirm full safety and accurate diagnosis of the mare's reproductive system through ultrasound.

Keywords: Ultrasound- Mares- Reproductive system - Ultrasonography.

Full-length article *Corresponding Author, e-mail: haithambarbary2005@gmail.com

1. Introduction

The early development of diagnostic ultrasound in equine veterinary medicine focused on cardiology, Theriogenology, and examining the abdomen and thorax. Ultrasonography is a rapid, accurate, harmless, and reliable diagnostic technique for directly imaging the reproductive organs' anatomy in situ and clarifying reproductive status [1]. It is an important diagnostic method for evaluating treatment regimens and ovarian and uterine diseases [2]. Its continuous use has recorded no damage to fertility or fetal abnormality [3]. In Arabian mares, a single reproductive ultrasound scan can yield more information, including detection of ovarian and uterine status, monitoring of ovarian and uterine pathology, monitoring of the postpartum mare, early pregnancy diagnosis, twin pregnancy detection, and determining ovulation time [4]. Endometritis and endometrial cysts were the most common abnormalities that ultrasonography could diagnose in barren mares. The hallmark signs of clinical endometritis determined by ultrasound are intrauterine fluid accumulation, especially after breeding [5]. Ultrasonography has been useful for diagnosing various ovarian abnormalities [6] and is probably the most common means of detecting glandular and lymphatic cysts [7]. Another application of reproductive ultrasonography involves conception, age, development, and viability [2].

This report presents the reproductive efficiency of mares subjected to routine ultrasound examination of the ovaries and the uterus during follicular growth and the early stages of gestation.

2. Material and Methods

2.1. Animals

Thirty Arabian mares from 16 to 23 years of age were subjected to reproductive ultrasound examination during three breeding seasons (March to June), from 2019 to 2021 on different stud farms in

Egypt.

2.2. Reproductive Examination

2.2.1 Ultrasound scanner

Sonoscape A5 has two dimensions and a 7.5 MHz central frequency transrectal probe made in China.

2.2.3. Ultrasound examination

Thirty Arabian mares were imaged by rectal ultrasonography to determine the estrous cycle stage, ovarian structures, and follicle and uterine echotexture measurements. Early to late pregnancy checks were also monitored. After entering the horse in his alley and being injected with a mild

tranquilizer if needed, the examination was carried out through the rectum using a fully lubricated transducer entered gently into the rectum after fecal evacuation. Ovaries, uterine horns, body, cervix, and vagina were scanned, and the different layers of the uterine wall (perimetrium, myometrium, and endometrium) were monitored.

Ultrasound examination could detect normal and abnormal reproductive findings. It also monitored the identification of the early and late stages of pregnancy.

3. Results

3.1. Ultrasonographic finding of the normal ovary

Mare ovary ultrasonically imaged as a kidney in shape containing nonechoic black circular follicles and/or echogenic irregularly shaped corpus luteum surrounded by echogenic white area (connective tissue stroma) as shown in Figure 1&2.

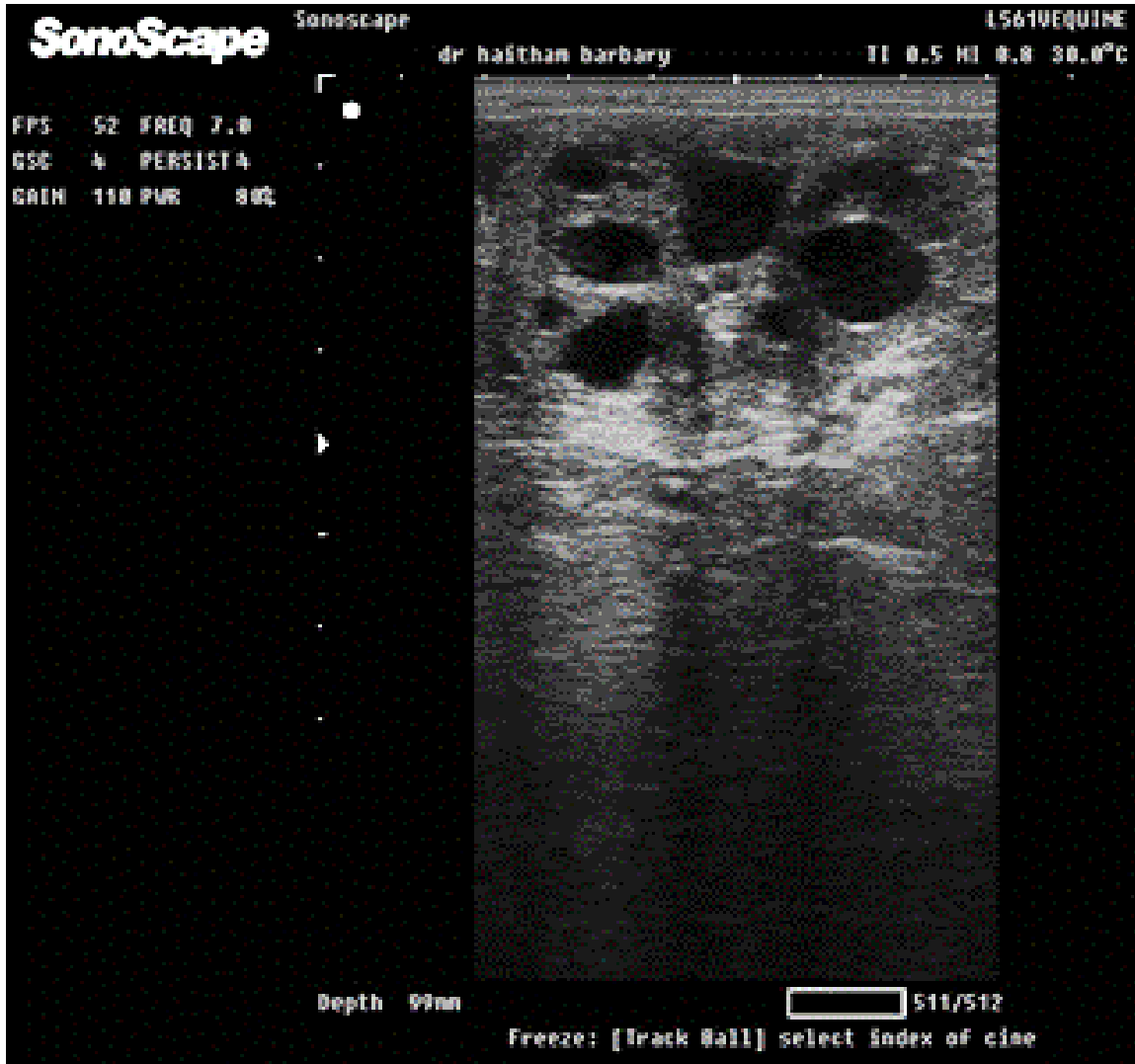


Fig 1: Ultrasonographic image of kidney shape ovary containing small follicles

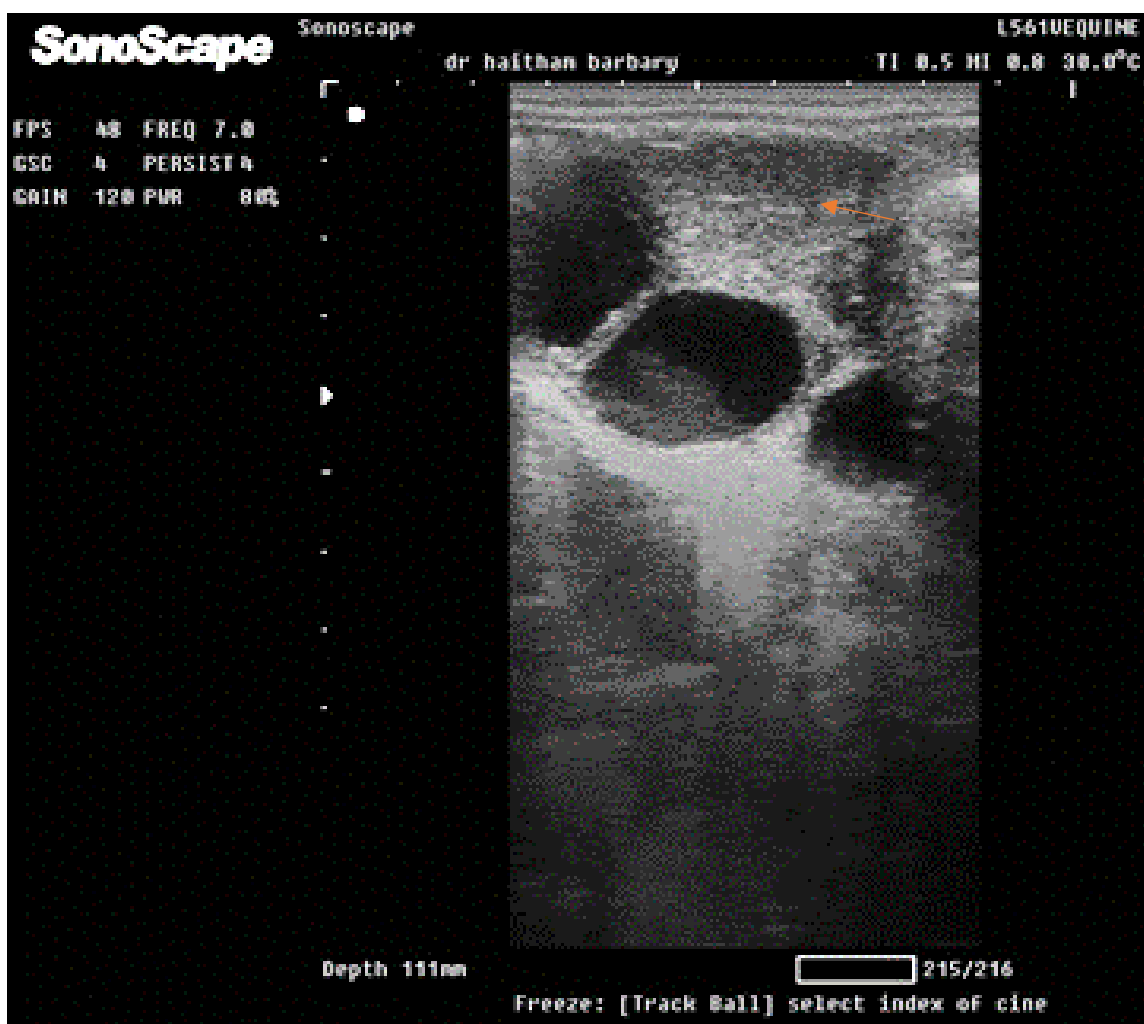


Fig 2: Ultrasonographic image of the ovary containing nonechoic (black) circular follicles and echoic CL (arrow)

3.2. Sonographic imaging of follicles

Follicles appeared as non-echogenic black areas that are spherical or irregular (Figure 3). Follicles grow at 2 to 2.5 mm per day. The preovulatory follicle is spherical with a thin hyperechoic wall, which changes to a flattened pear or irregular shape seen as ovulation approaches in association with a hyperechoic thick wall, hyperechoic dots at the bottom of follicle peripheral nonechoic or hypoechoic line could be seen around the follicle (Figure 4&5). normal ovulatory follicular size lies between 3.5 and 5.7 mm in diameter.

3.3. Sonographic Imaging of corpus hemorrhagicum and corpus luteum

As the fluid is released, the follicle changes from anechoic to a heterogeneous appearance at ovulation. During 24- 48 hours following ovulation, the corpus hemorrhagicum

formed from the peripheral hyperechoic luteinized tissue zone and central hypoechoic blood clot zone, which may have fibrin threads (Figure 6). During diestrus, the corpus luteum was irregular, with two luteal morphologies monitored in examined mares; compact CL had a homogenous echogenicity (Figure 7), and the corpus luteum had a nonechoic central cavity.

3.4. Sonographic finding of non-pregnant uterus

As the transducer was held in a sagittal plane, the cervix and uterine body were imaged longitudinally, but the uterine horn was seen in cross sections as the transducer was moved left or right. Ultrasonically, the cross-section of the uterine horn was divided into three layers. The first one was the perimetrium (outer peritoneal border), the second was the hypoechoic area from the perimetrium to the endometrium (myometrium), and the third was the endometrium, which was imaged as a hyperechoic line lying in the center of the uterus (Figure 8).



Fig. 3: Ultrasonographic image of the spherical preovulatory follicle



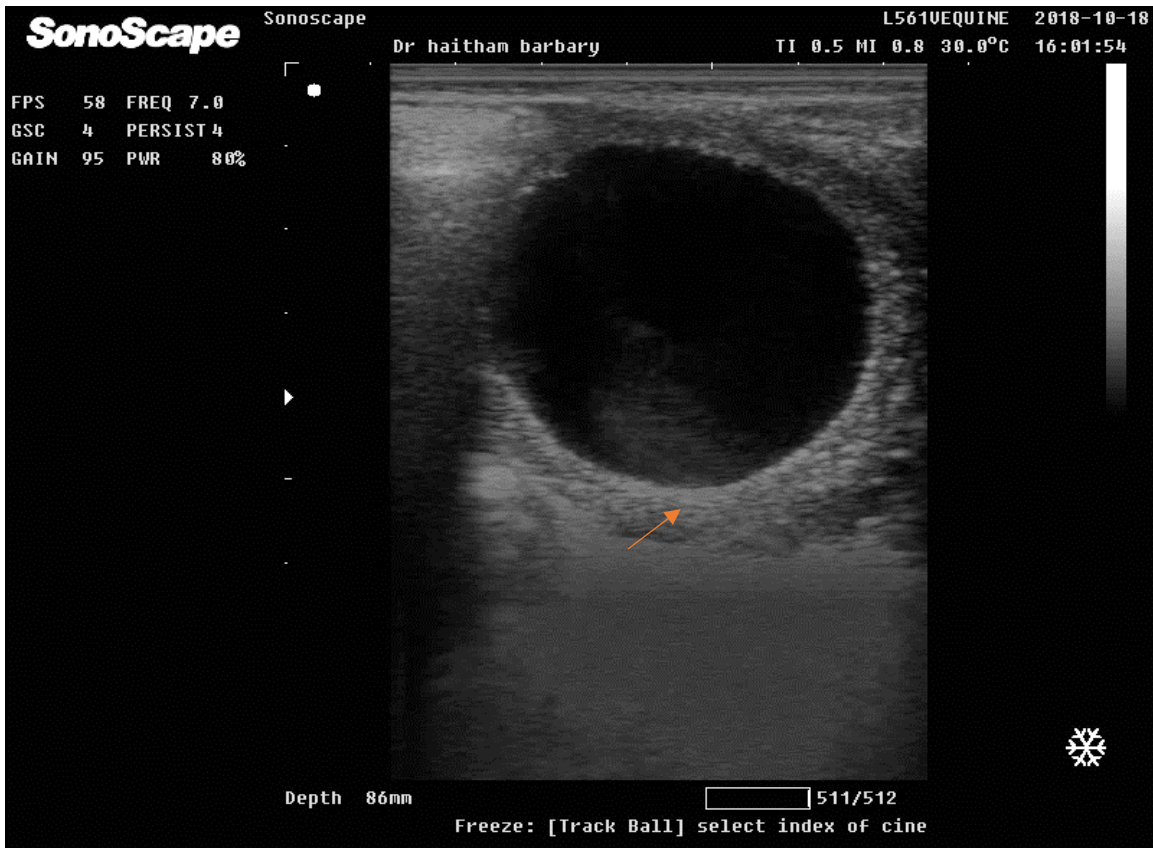


Fig. 5: Ultrasonographic image of ovulatory follicle showed a hyperechoic thick wall (arrow)

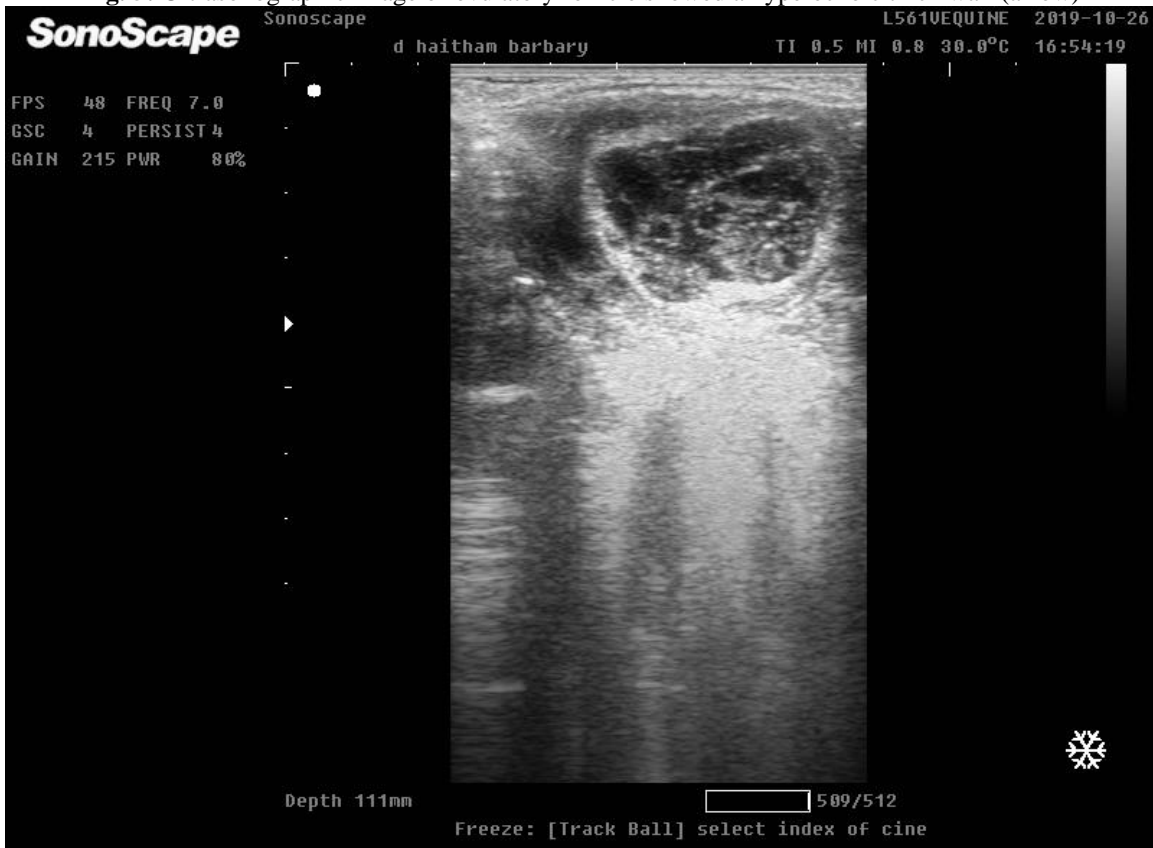


Fig. 6: Ultrasonographic image of corpus hemorrhagicum 48 hours following ovulation

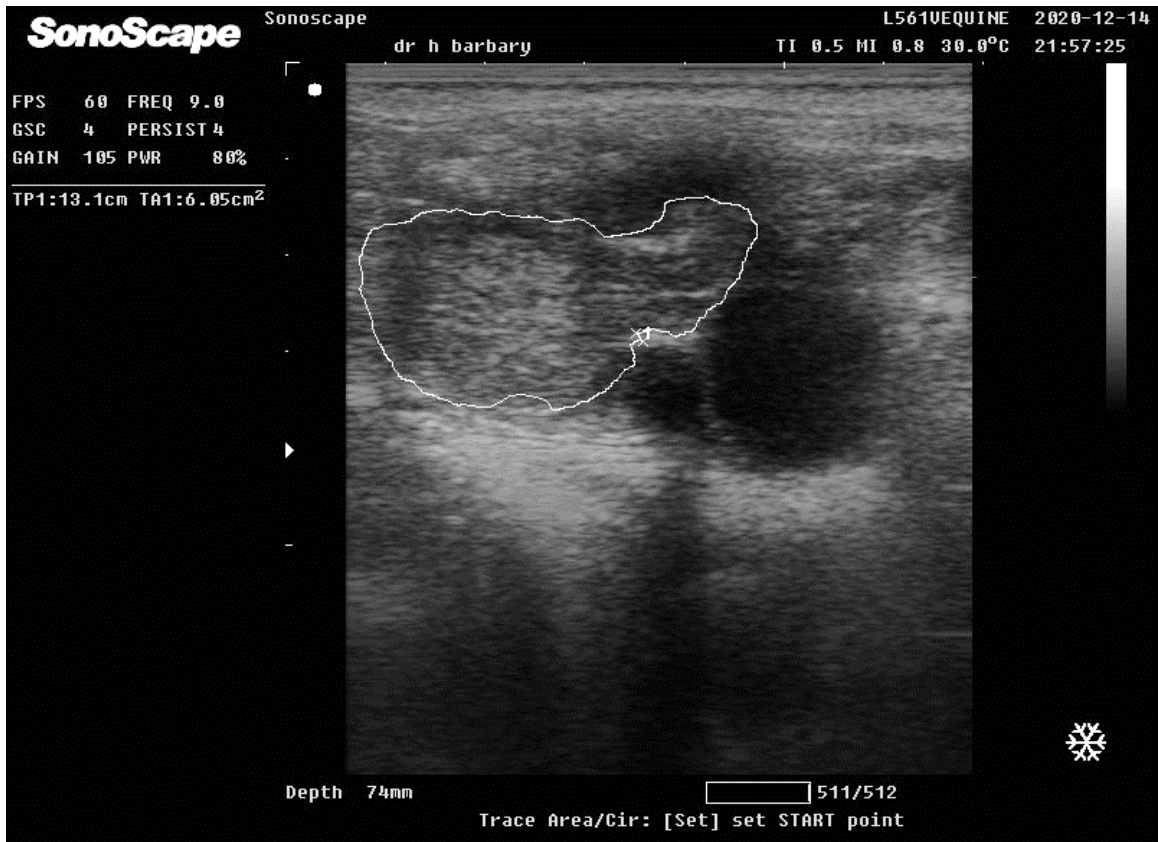


Fig. 7: Ultrasonographic image of compact CL

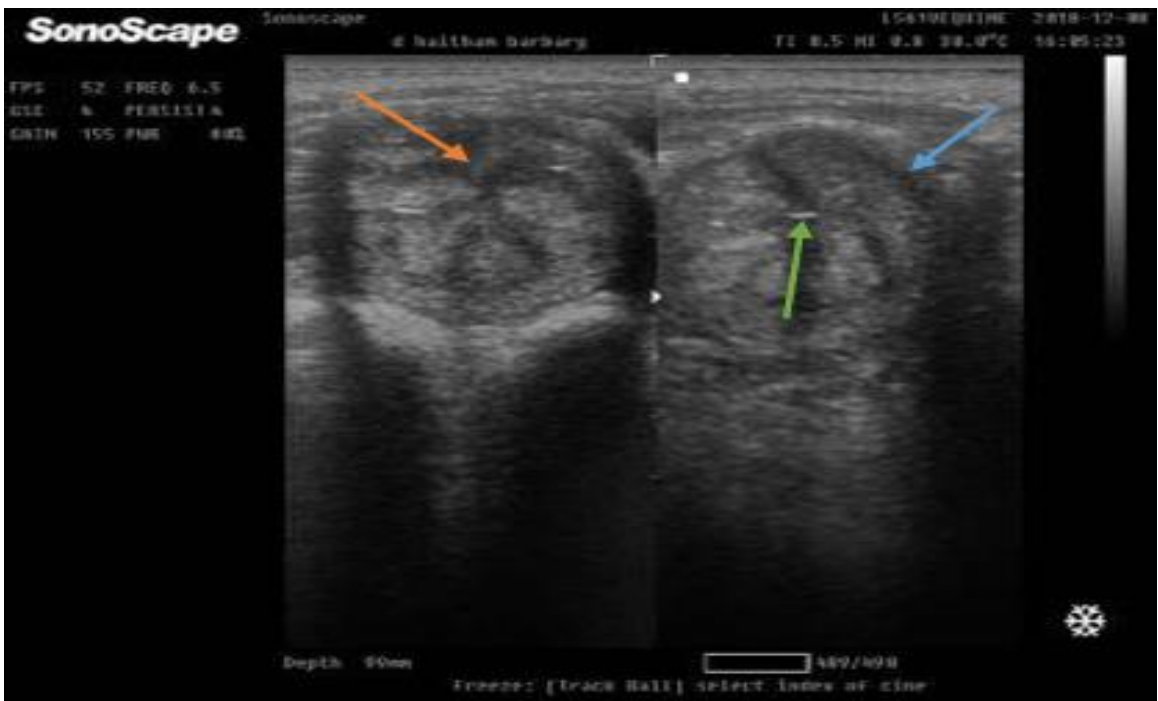


Fig. 8: Cross-section through LF and RT uterine horn. Note the hypoechoic peritoneal border (blue arrow), gray color myometrium (orange arrow), and the hyperechoic spot (green arrow) endometrium.

3.5. Sonographic imaging of estrus uterus

The uterus has a heterogeneous echotexture appearance on the ultrasound screen, with prominent endometrial folds due to endometrial edema. The uterine body has a characteristic leaf-like or starfish appearance, and the uterine horns' cross-sectional images show a wheel-shaped appearance (Fig. 9&10).

3.6. Sonographic imaging of diestrus uterus

On the ultrasound screen, the uterus has a homogenous echotexture appearance, with non-prominent endometrial folds (Figure 11, 12).

3.7. Sonographic finding of pregnant uterus

Ultrasonography has provided a means to visualize all phases of embryo development and viability, which are divided into three phases: The Yolk sac phase (days 11–20), the allantoic sac phase (days 21–40), and the Fetal stage (imaging of the fetus and the fetoplacental unit from day 40). In the yolk sac phase, the embryonic vesicle can first be detected on day nine and visible as a fluid-filled anechoic sphere found more frequently in the body at this stage. The rapid growth of the embryonic vesicle occurs until 16 days and is associated with a change in the shape of the vesicle from spherical to oval, to triangular; it then becomes irregular in outline located at or near the corpus–corneal junction. From early detection of the embryonic sac to 16 days, a bright white (echoic) spot was observed on the dorsal and ventral aspects of the yolk sac image called specular artifact, which was characteristic of an embryonic vesicle, where the sound waves impact vertically on its front and back walls—estimated conceptus age during this stage by measurement of sac diameter which is called gestational sac diameter GSD (Figure 13 to 20). The allantoic sac phase is characterized by an enlarged and irregularly shaped embryonic vesicle. By d 22, the embryo is properly detected at the sac bottom (a hyperechoic spot), embryonic development has been increased and clarified, the embryo ascends and descends within the sac, and the associated development of the umbilical cord can be seen. The embryonic vesicle height is not a reliable indicator for estimating the day of pregnancy due to periodic shifts in the allantoic fluid that begin to occur. Thus, fetal body length (crown rump length) CRL is used to estimate the day of pregnancy. Also, the embryo's proper heartbeat can be visualized by d 22 of pregnancy at this stage (Figure 21 to 24). By day 40 to 60 of pregnancy, the embryo was imaged ultrasonically as a hyperechoic mass and positioned near the bottom of the embryonic sac with a prominent umbilical cord attached to the dorsal pole of allantochorion (Figures 25, 26, and 27). The trunk diameter was taken to determine the fetal age. The prominent structures of the fetus, such as the head, the eye, and the cranial cavity, were detected until day 335 of pregnancy when a prominent placenta could be seen. The

eyeball diameter (EBD) was taken to determine the fetal age (Figures 28& 29).

3.8. Ultrasonographic imaging of endometritis uterus

We found 27 aged Arabian mares had reproductive problems out of 30 examined mares, with a percentage of 90%. This high percentage of uterine problems is due to aging (more than 15 years old). From 27 reproductive problems mares, there were 17 (56.6%) bacterial endometritis mares (determined by bacteriological uterine culture), and 10 (33.3%) uterine cysts cases (Figure 30). The accumulated intraluminal fluid with different echogenicity was the hallmark sign of uterine inflammation that could be seen during estrus in all 17 mares. Also, all 17 mares were conducted for uterine bacteriological examination, and the infection was confirmed. Also, all 17 mares were conducted for uterine bacteriological examination, and the infection was confirmed. Accumulated ILF is imaged as mobile, free, fluid-filled areas with poorly defined borders within the uterine body or horn, ranging from non-echoic to hyperechoic echotexture. Figure 31 (A, B) showed the ultrasonic difference between the normal uterine body echotexture and endometritis mare. A cross-section of the uterine horn with accumulated ILF appeared in Fig. 32. Stellate-shaped fluid outline with bulged prominent endometrial folds into a lumen with a wavy uterine wall. All endometritis-diagnosed mares (n=17) had ILF (1 to 4 grades) during estrus except one mare that accumulated fluid during the diestrus (Figure 33). According to ultrasound echogenicity, the intrauterine fluid detected was graded into black nonechoic grade I, gray hypoechoic with white hyperechoic dots grade II, homogeneously distributed gray moderately echogenic grade III, and grade IV white hyperechoic (Figure 4-34, 4-35& 4-36). Grade I intrauterine fluid accumulation was detected in 9 cases, 4 cases diagnosed in grade II, and 3 cases diagnosed in grade III accompanied by bacterial endometritis. Only one case had Grade IV ILF during diestrus (Figures 34 a, b, c, d).

3.9. Ultrasonographic imaging of uterine endometrial cyst

We found ten aged Arabian mares with uterine cysts from 30 examined mares, with a percentage of 33.3% of total mares and 37% of reproductive abnormalities mares. Total number of lesions referred to 3 cases from 27 infertile mares found to have more than one uterine lesion endometritis and uterine cyst (Figure 35). The uterine cyst is ultrasonically visible as single or multiple fluid-filled structures with varying sizes and shapes coated with echoic membrane. A single uterine cyst may be exactly similar to an embryonic vesicle. Also, most detected endometrial cysts were multiple; the largest size was a grape cluster (Figure 36 a, b). In uterine cysts with endometritis cases, an ultrasound screen was imaged as a clear, thickened hyperechoic wall circular or irregular structure floated within the accumulated intrauterine fluid (Figure 37 a, b, c, d).



Fig. 9: Ultrasonographic image of the estrus uterus (CS) note prominent endometrial folds (arrow).



Fig. 10: Ultrasonographic image of uterine body (LS) with leaf-like appearance during estrus



Fig. 11: Ultrasonographic image of the horn (CS) during diestrus homogenous appearance.

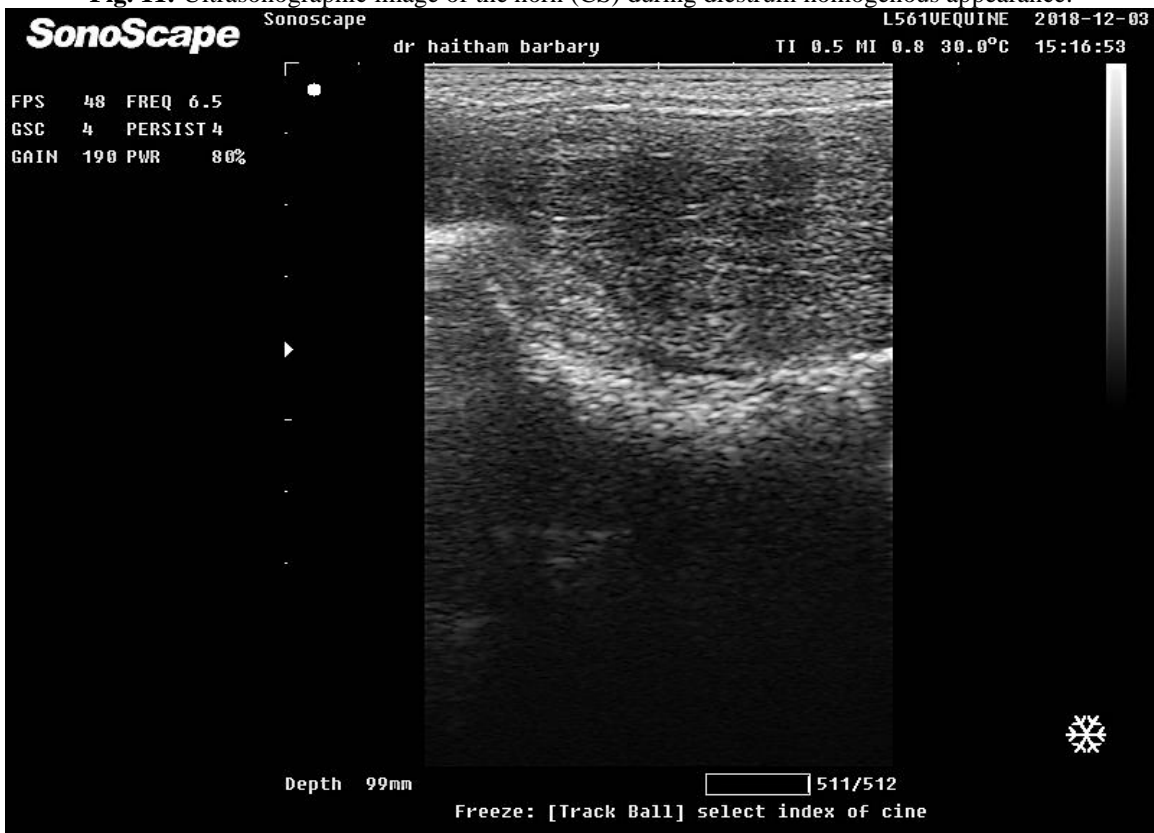


Fig. 12: Ultrasonographic image of the uterine body (LS) during diestrus

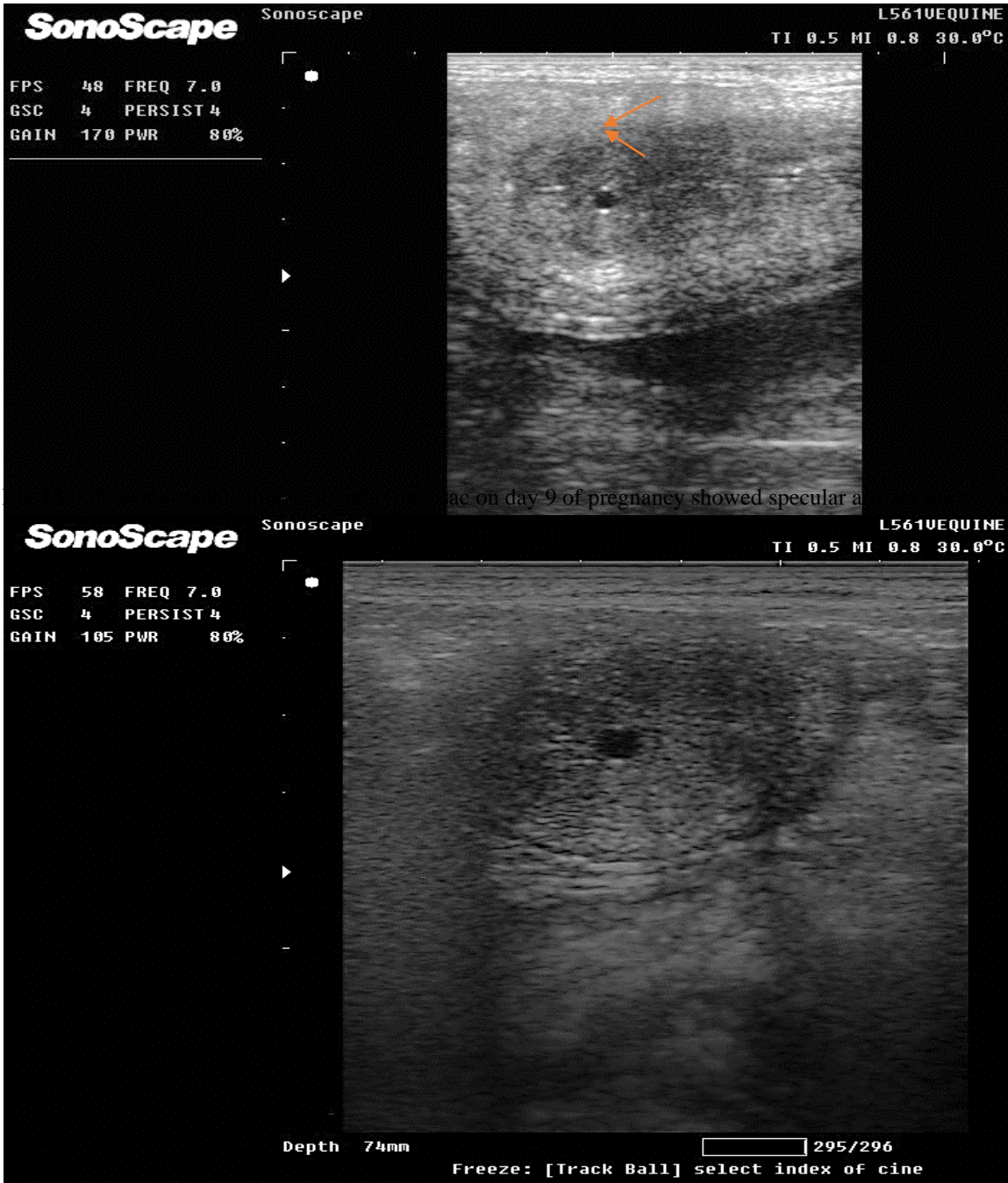


Fig 14: Ultrasonographic image of embryonic sac on day 10 of pregnancy



Fig 15: Ultrasonographic image of embryonic sac on day 11 of pregnancy



Fig 16: Ultrasonographic image of embryonic sac on day 12 of pregnancy.

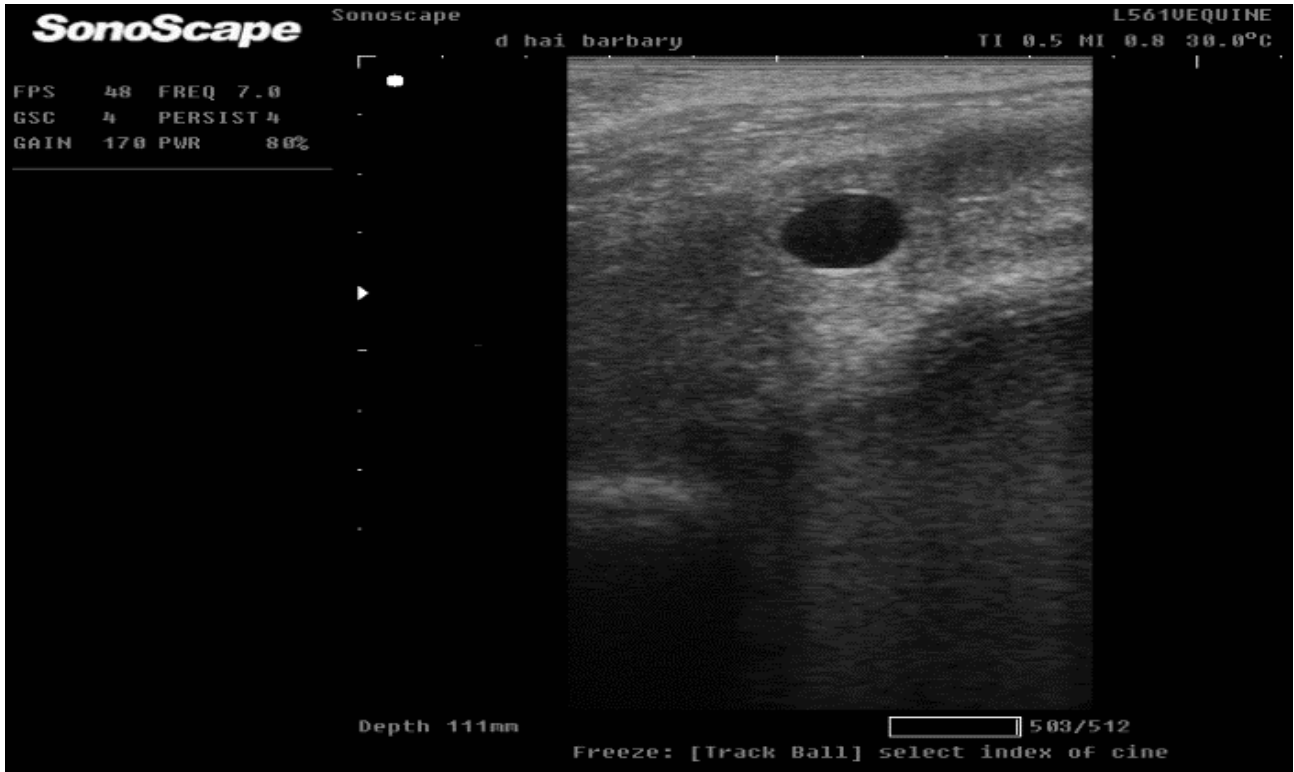


Fig 17: Ultrasonographic image of embryonic sac on day 13 of pregnancy.



Fig 18: Ultrasonographic image of embryonic sac on day 16 of pregnancy.



Fig 19: Ultrasonographic image of embryonic sac on day 19 of pregnancy showed loss of specular artifact and irregular shape sac.

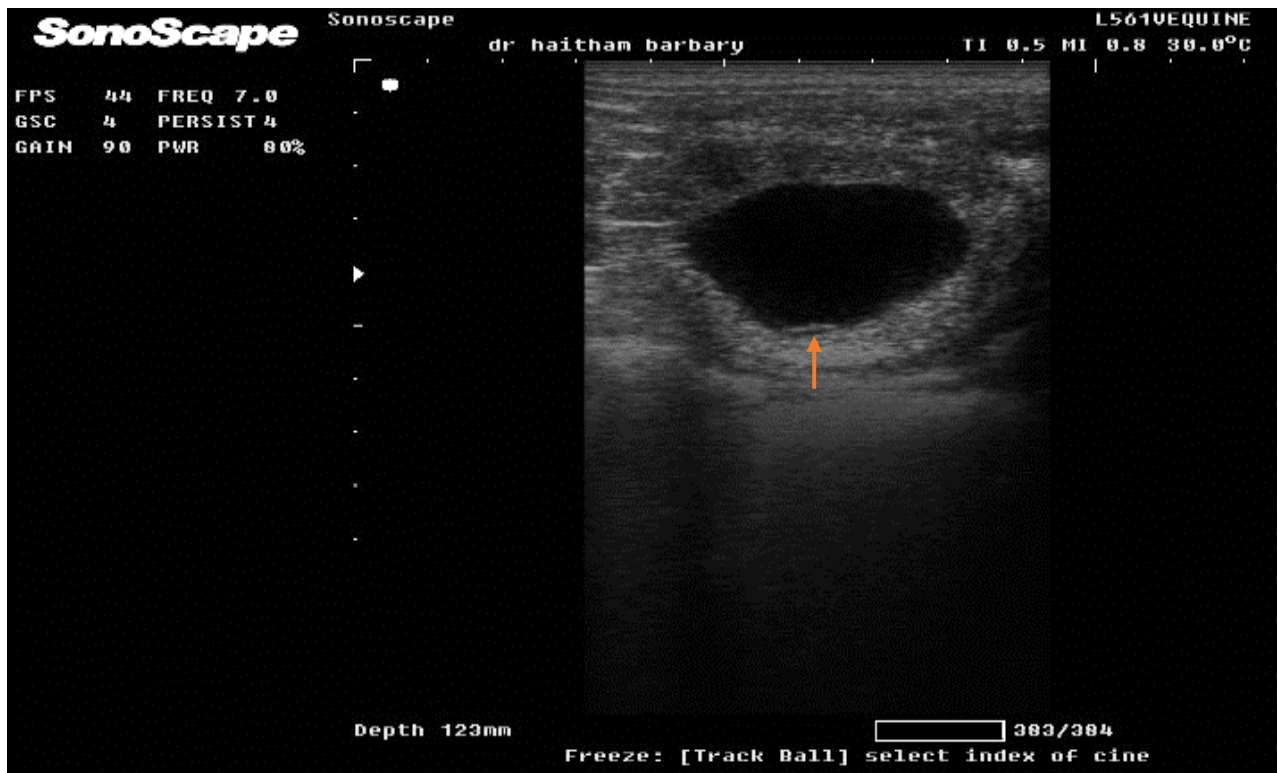


Fig 20: Ultrasonographic image of the embryonic sac on day 20 of pregnancy showed a hyperechoic embryonic mass at the bottom of the sac (arrow).

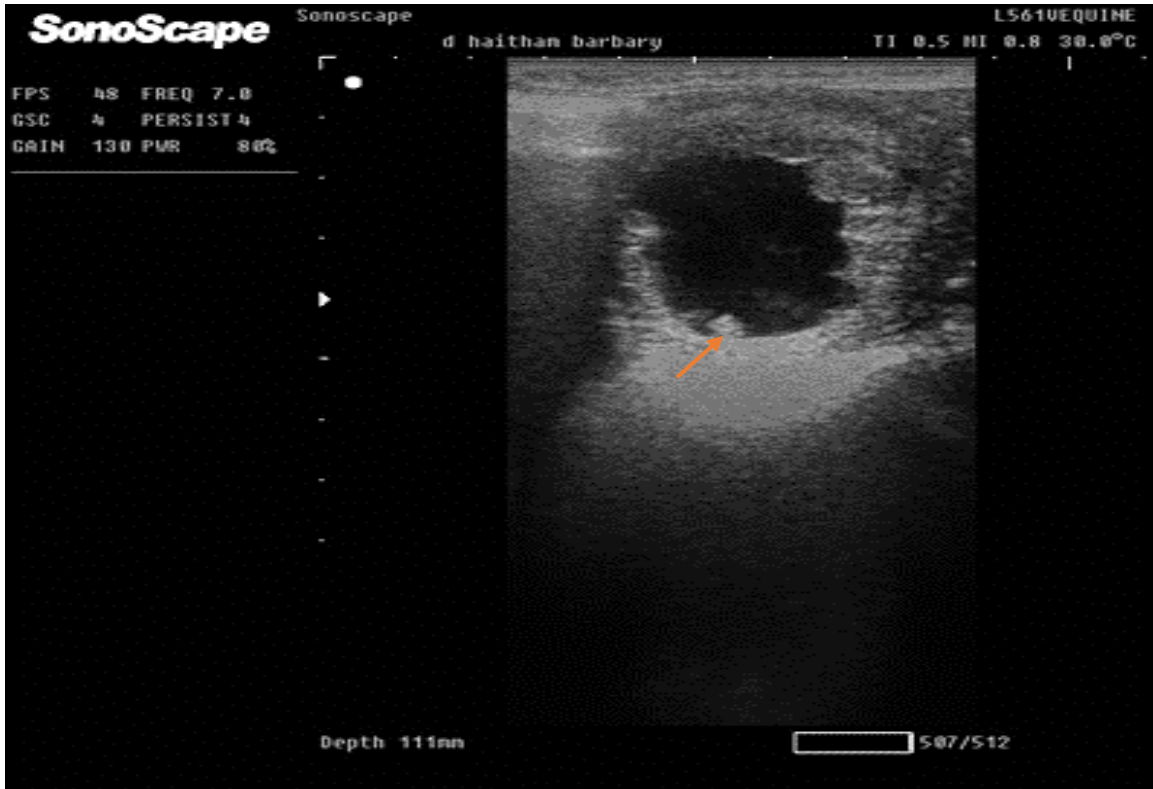


Fig 21: An Ultrasonographic image of the conceptus on day 22 of pregnancy showed a non-echoic sac, with an echoic mass embryo at the sac's floor (arrow).



Fig 22: An ultrasonographic image of the conceptus on day 27 of pregnancy showed the ascent of the embryo and ventrally positioned allantois (arrow).



Fig 23: Ultrasonographic image of conceptus on day 30 of pregnancy showed the embryo in the sac center.



Fig 24: Ultrasonographic image of conceptus on day 36 of pregnancy measured by CRL diameter. The embryo is suspended high in the embryonic sac (arrow).

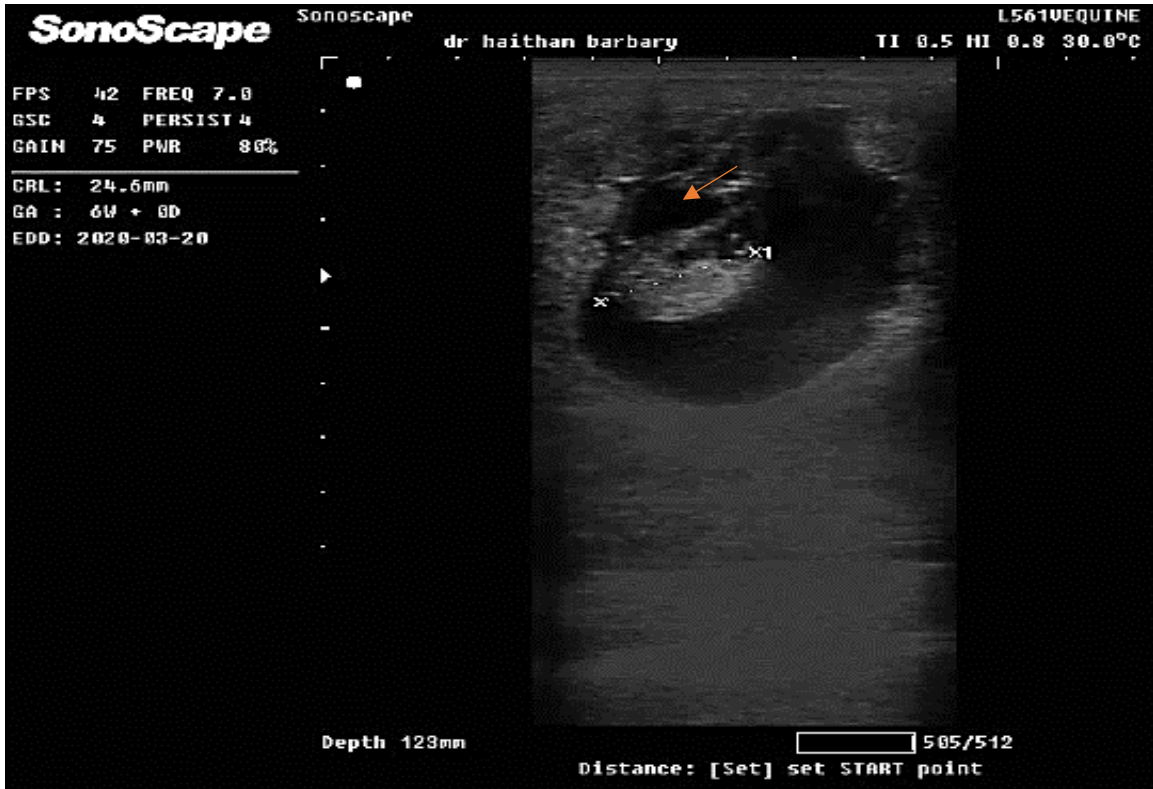


Fig. 25: Ultrasonographic image of conceptus on day 42. The embryo descends over the sac floor and is hung with an umbilical cord. The remnant of yolk still could be seen (arrow).



Fig 26: An ultrasonographic image of the conceptus on day 50 of pregnancy showed the embryo's (CS) near the sac floor (arrow).



Fig 27: Ultrasonographic image of conceptus on day 47 of pregnancy showed a prominent umbilical cord (arrow).



Fig 28: Ultrasonographic image of the fetus (arrow) on day 100 of pregnancy. The hyperechoic bone of the fetus and the prominent placenta (blue arrow) could be seen.

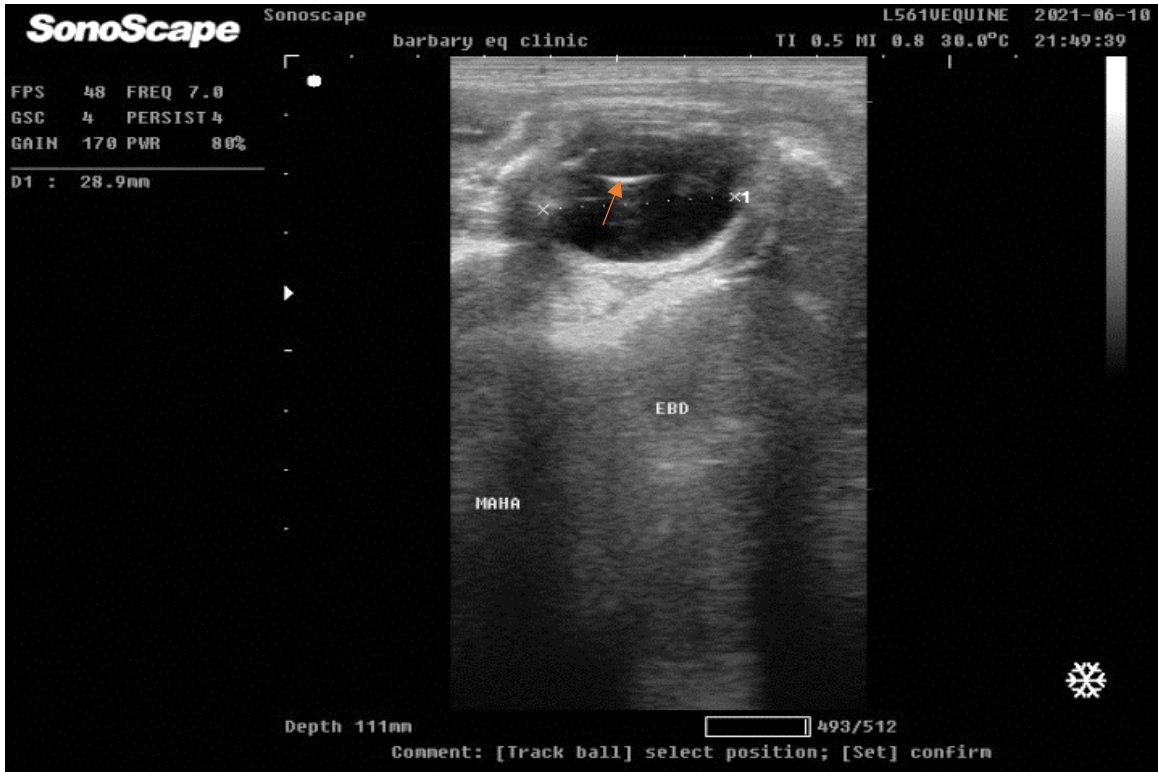


Fig 29: Pregnancy on day 210. eye lens (arrow) is depicted, and the EBD is measured.

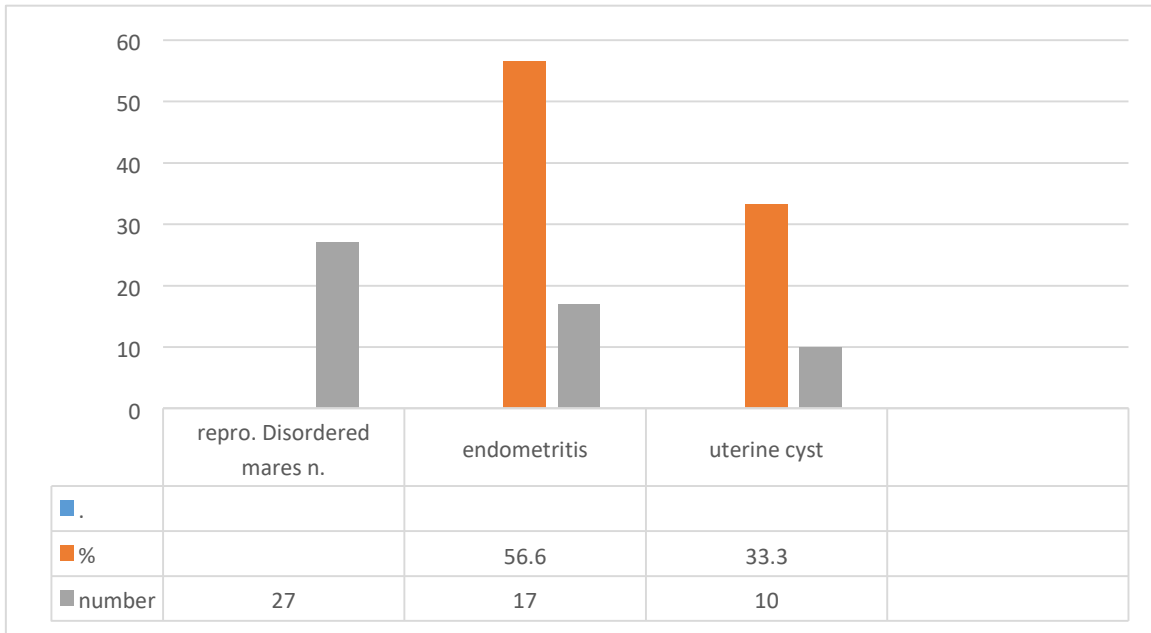


Fig. 30: Incidence of different types of reproductive disordered mares.



Fig. 31 A: Longitudinal section of the normal uterine body of a mare without fluid accumulation.



Fig. 31 B: Ultrasonographic image of the uterine body of a mare with fluid accumulation

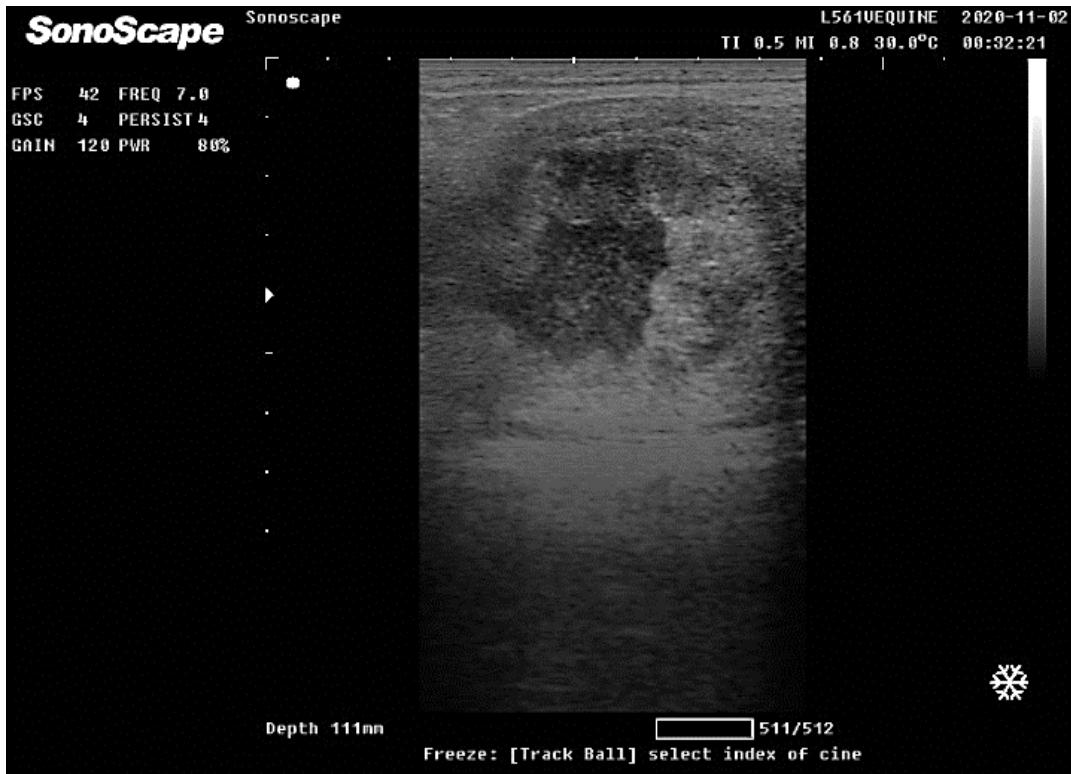


Fig. 32: Ultrasonographic image of horn (CS) of a mare with endometritis. The lumen contains a moderate amount of exudate, and the endometrial folds bulged into the lumen.

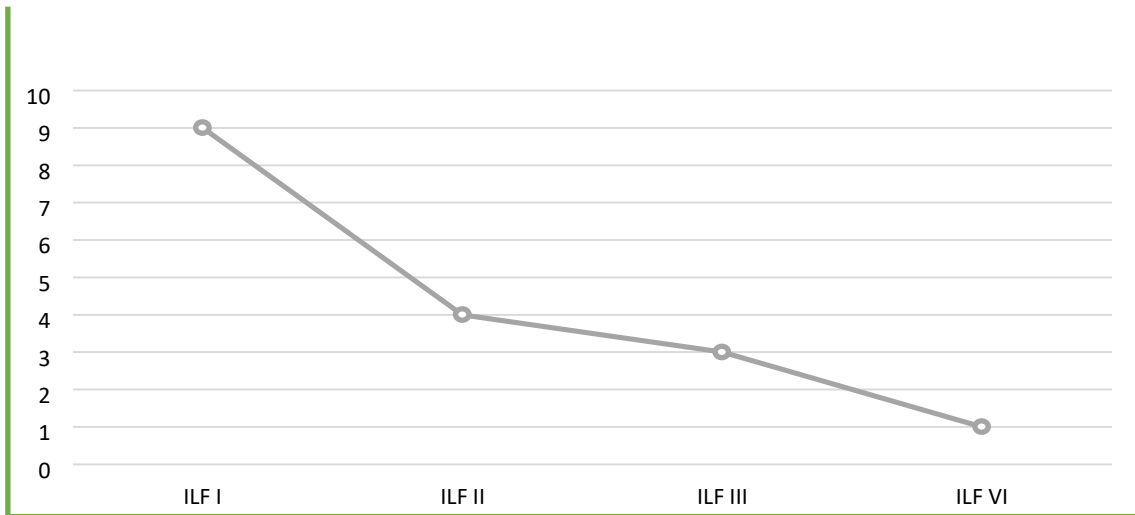
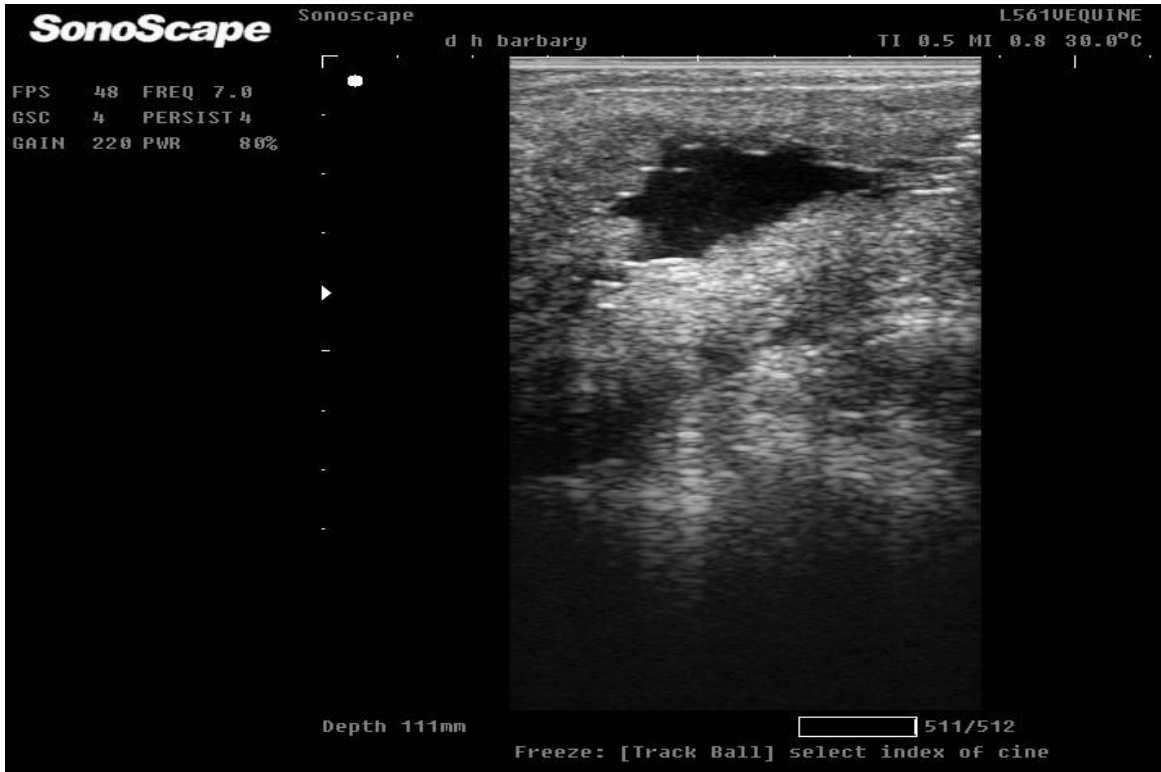


Fig. 33: Incidence of different grades of ILF accumulated in examined infertile mares.



A: GI nonechogenic black color



B: GII Hypoechoic with hyperechoic dote



C: GIII moderately echogenic



D: GIV hyperechoic

Fig. 34: Ultrasonographic imaging of different grades of intraluminal uterine fluid

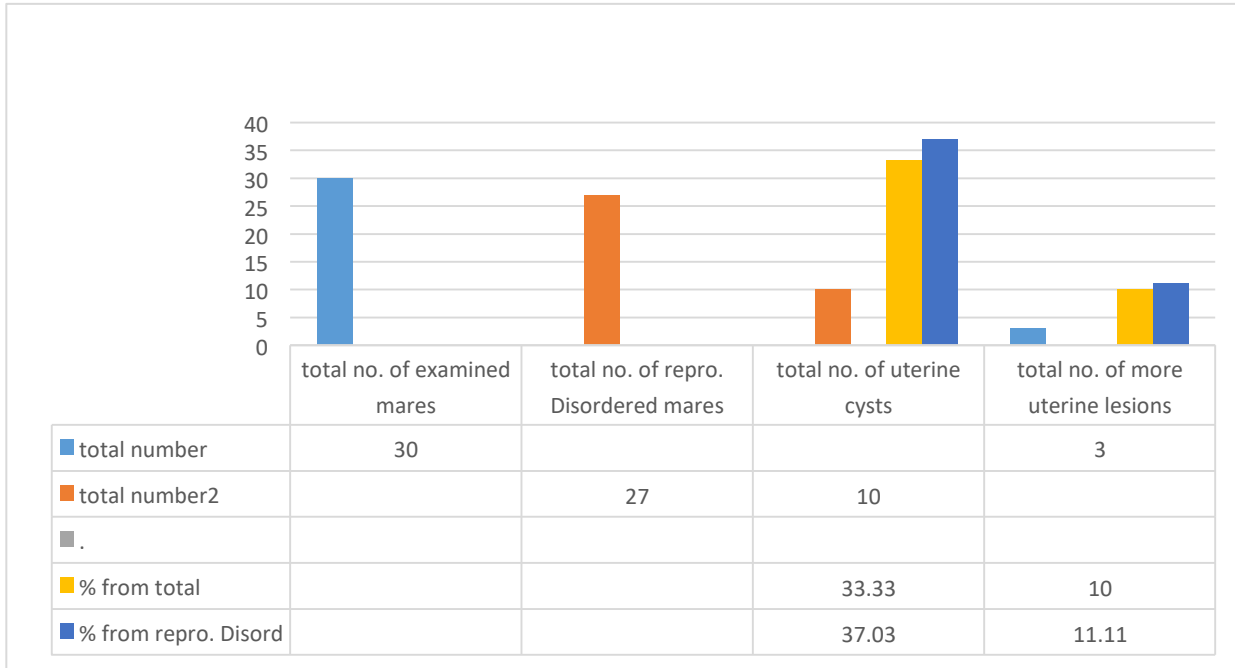


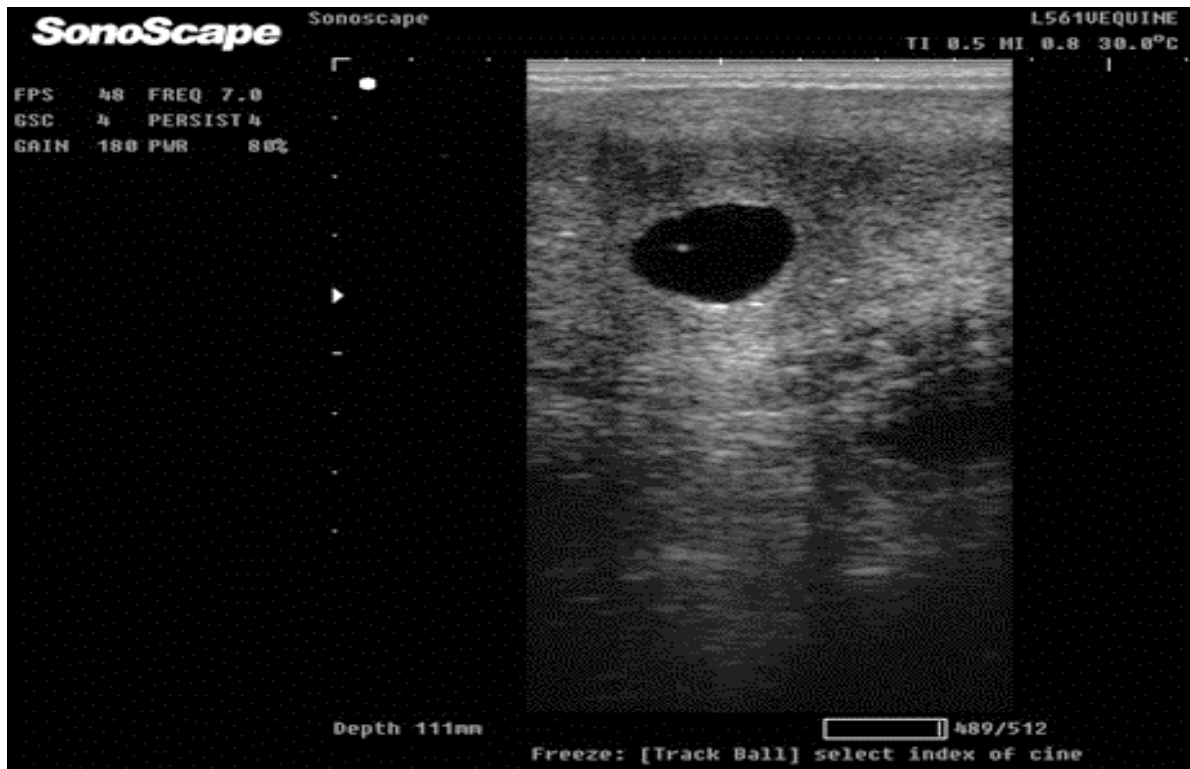
Fig. 35: Incidence of uterine cysts among total number and reproductive disordered mares.



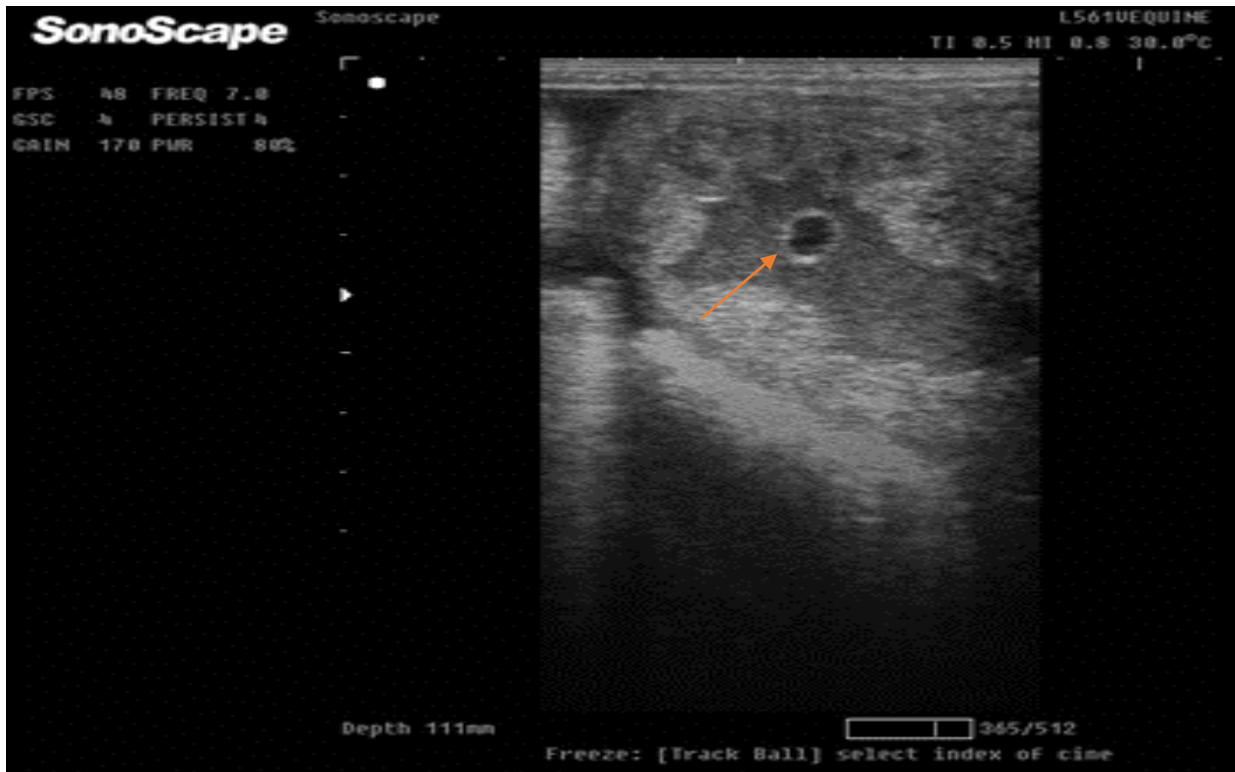
35-a: Large-sized single uterine cyst measured 56.1mm in the uterine body



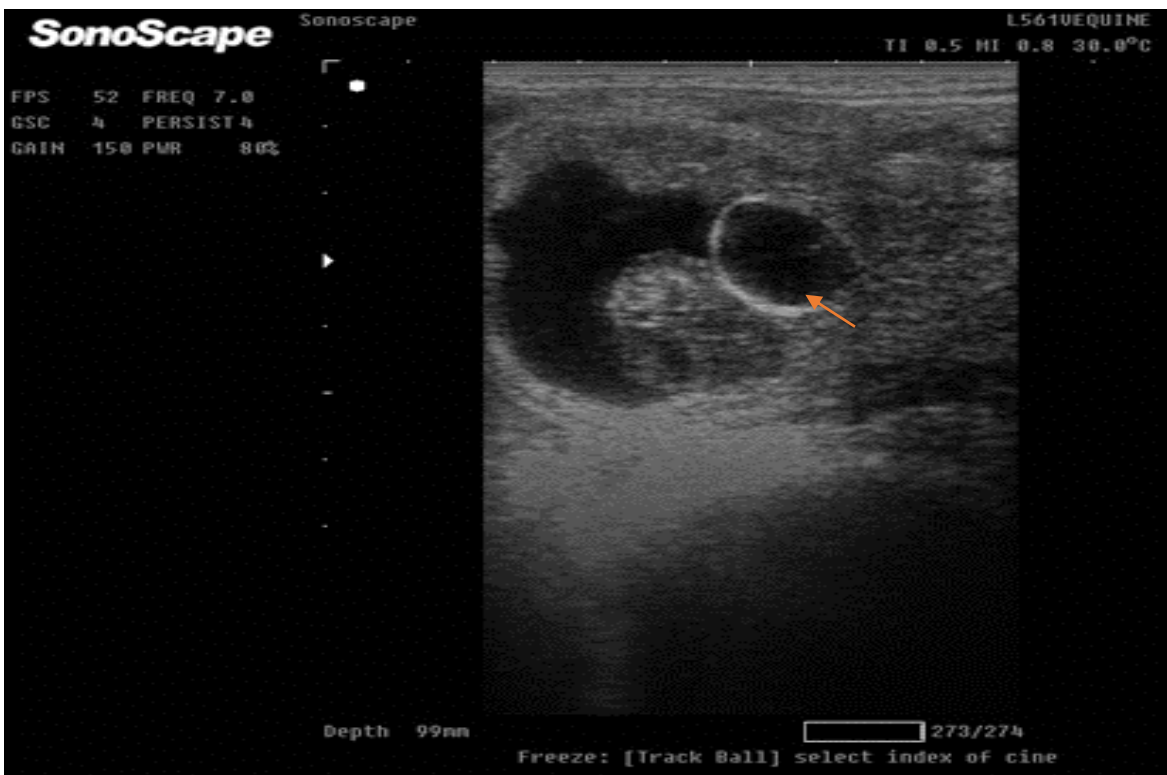
35-b: multiple grape cluster endometrial cysts in the uterine body.



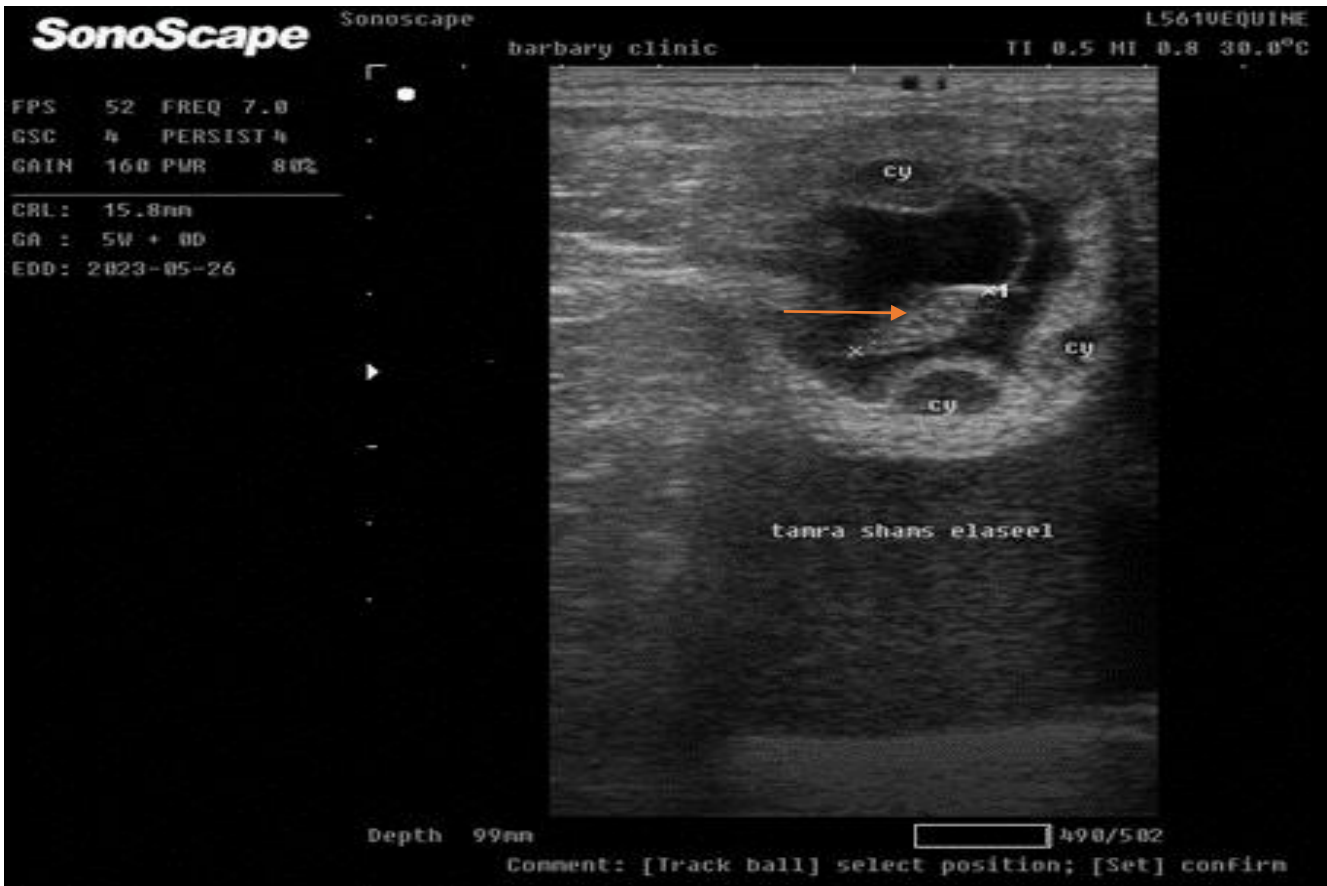
36-a: Single uterine cyst resembling an embryonic sac.



36-b: circular- shaped uterine cyst (arrow) floating in accumulated uterine fluid.



36-c: A large-sized cyst (arrow) pressed on the embryonic sac with the embryo proper could be seen.



36-d: multiple cysts around embryonic sac with 35 days-aged embryo (arrow).

4. Discussion

Ultrasonography is useful for evaluating normal and abnormal findings of genital organs. In the present study, [1,2] stated that ultrasonography is one of the most accurate and rapid methods for evaluating equine reproductive patterns. In the current study, sonographic images of ovarian follicles appeared as a spherical anechoic black structure with a thin hyperechoic wall (preovulatory) that changed to an irregular shape with the wall becoming thicker hyperechoic (ovulatory). These findings agreed with [8], who showed that on the ultrasound viewing screen, the follicles changed from a circular to an oval shape with an increase in wall thickness when the interval to ovulation decreased. In our work there are two luteal morphologies could be seen in mares: solid corpus luteum with homogenous echogenicity and corpus luteum that developed central cavity (corpus hemorrhagicum), which consists of the hyperechoic peripheral zone of luteinized tissue and hypoechoic central zone of blood clot detected during 24- 48 hours after ovulation. Similar results were obtained by [9] They found that after the follicle ruptures, a corpus hemorrhagicum forms. It has one of two appearances on the ultrasound screen. The first one is either a uniformly echogenic image or contains a centrally non-echogenic center. Echogenic lines may be attributable to clotting and fibrinization in the central nonechogenic center. The current study differentiated the cross-section ultrasound image of the uterine horn during the estrus and diestrus. The diestrus uterus is a relatively homogeneous echotexture. Barbary, 2023

During estrus, the uterus has a very heterogeneous appearance (a mixture of hyperechoic and hypoechoic areas), forming a wheel appearance. This ultrasonic appearance results from endometrial edema [6,10]. They stated that ultrasonic echotexture changes according to the degree of the endometrial fold's edema. Estrous echotexture is characterized by hyperechoic connective tissue core and hypo-echogenic edematous outer area of the endometrial folds. A homogenous appearance without any edema or prominence of endometrial folds characterizes the diestrus uterus. In the current study, the embryonic vesicle was detected on day nine and characterized by a fluid-filled anechoic (black) typically circular structure with characteristic hyperechoic white spots that formed specular artifacts. Growth of the embryonic vesicle occurred from 9 to 19 days and was associated with an apparent change in the shape from spherical to oval, triangular, or irregular in outline. At 21 days, the embryo proper could be seen as a small echogenic mass in the sac bottom, whereas we see the fetal pulse at 22 days of pregnancy. Also, at this stage, ultrasound estimation of conceptus age could be made using gestational sac diameter. The same results were reported by [6,10]. From 22 to 45 days of pregnancy, the ultrasound scanning in our study revealed increased embryo proper development and diameter with a change in the percentage of the embryonic vesicle occupied by yolk versus allantoic fluid. At 25 days, the allantois occupied 25% of the embryonic vesicle, 50% of the vesicle at 30 days, 75% at 35 days, and nearly 100% at 40 days. At this stage,

ultrasound estimation of conceptus age could be made using crown-rump length. Also, by ultrasound examination on day 54 of pregnancy, the fetus lay on the floor of the vesicle, and several features of the fetus were detected. At the last stage of pregnancy, the ultrasound imaging of fetal organs can be detected as imaging of the fetal eyeball, which appeared as an anechoic black vitreous body surrounded by a hyperechoic orbit, and the lens could be detected as a hyperechoic line. At this stage, ultrasound estimation of conceptus age could be made by bi-parietal and eyeball diameter. Nearly similar to our results were reported by [11] who stated that by day 45 of pregnancy, the fetus and the umbilical cord were visible. Also, the late-term fetus and its uteroplacental unit could be imaged by ultrasonography [12]. In the present study, 17 (56.6%) aged Arabian mares were diagnosed with bacterial endometritis. Nearly similar results were reported by [4], who mentioned that 69% of subfertile mares had bacterial endometritis diagnosed by ultrasound and bacterial uterine culture. Also, [13] reported that bacterial endometritis is the main loss in equine breeding industries, representing 25–60% of barren mares. In our work, the only recognized ultrasound feature of endometritis suffered by mares was intraluminal uterine fluid accumulation. On the same line, Ferris et al. (2014) summarized that fluid collection in the uterus is the main symptom of uterine inflammation. Intrauterine fluid was graded by ultrasonography into four grades: black nonechoic grade I, gray hypoechoic with white hyperechoic dots grade II, homogenous distributed gray moderately echogenic grade III, and white hyperechoic grade IV. [11] also reported that we grade ILF accumulation by ultrasound according to echogenicity from grade I to grade VI. In our work, there were ten mares from total uterine abnormalities mares (n=27), with a percentage of 33.3% having endometrial cysts. However, a slightly lower incidence of uterine cysts was reported by [14] who concluded that the expected occurrence of cysts in a population of subfertile Arabian mares is 28%. Our findings show that ultrasonography allows an accurate and reliable method for uterine cyst diagnosis. On the ultrasound screen cysts were imaged as a single or multiple immobile irregularly shaped fluid-filled non-choic structure with a thick hyperechoic wall. The shape of cysts varies from spherical or oval to irregular in outline and, in some cases, looks like embryonic vesicles. [15] mentioned the same results.

5. Conclusions

Ultrasonic imaging is a noninvasive and non-disruptive tool for evaluating normal and abnormal reproductive organs in straight Egyptian Arabian mares. As such, it provides the opportunity for reproductive status that were previously unknown and unobservable. Also, in contrast to traditional methods, ultrasonography permits a much earlier and more accurate diagnosis of pregnancy without any hazard to embryonic formation. Uterine inflammation and cysts are the only causes of subfertility, occurring in 90% of aged straight Egyptian Arabian mares in the present study. Intrauterine fluid accumulation is indicative of inflammation associated with subfertility and related to early embryonic death. Ultrasound is a valuable, reliable diagnostic tool for detecting intrauterine fluid accumulation. As such, it provides location, size,

echogenicity, and degree of fluid accumulation. I concluded that ultrasound is the key to the reproductive field of horses, as it is the pillar for diagnosing and following up on mares' reproductive conditions, thus increasing the equine reproductive industry and horse production.

References

- [1] P.M. Fricke. (2002). Scanning the future-ultrasonography as a reproductive management tool for dairy cattle. *J. Dairy Sci.*, 85: 1918- 1926.
- [2] P.G. Griffin & O.J. Ginther. (1992). Research applications of ultrasonic imaging in reproductive biology. *J. Anim. Sci.*, 70: 953-972.
- [3] Ginther, OJ. (1986): Ultrasonic imaging and reproductive events in the mare. *Equiservices Publishing; Cross Plains, WI*, PP. 338-340.
- [4] H.A. Barbary, I.I Abo-ghonema, I.E. El-Bawab &M.S. Fadel, (2016). Using of ultrasonography in evaluating the reproductive status in mares. *Msd. Thesis, Fac. Vet. Med., Damanhur Univ.*
- [5] M.M. LeBlanc & R.C. Causey. (2009). Clinical and Subclinical Endometritis in the Mare: Both Threats to Fertility. *Reprod Dom Anim*, 44 (3): 10–22.
- [6] T.L. Blanchard, D.D. Varner, J. Schumacher, C.C. Love, S.P. Brinsko & S.L. Rigby. (2003). Transrectal Ultrasonography in Broodmare Practice. In: *Manual of equine reproduction.2nd E.d., Philadelphia, PA, USA*. PP. 43-57.
- [7] M.B. Stanton, J.V. Steiner & D.G. Pugh. (2004). Endometrial Cysts in the Mare. *J Equine Vet Sci*, 24:14-19.
- [8] E.L. Gastal, M.O. Gastal, and O.J. Ginther, (1998): The suitability of echotexture characteristics of the follicular wall for identifying the optimal breeding day in mares. *Theriogenology*, 50:1025-1038.
- [9] M. LeBlanc, C. Lopate, D. Knottenbelt, and R. Pascoe, (2003): The mare. In: *Equine stud farm medicine and surgery. 1st E.d., London, Elsevier*, PP. 113-225.
- [10] W. Kahn. (1994). Ultrasonography in the mare. In: *Veterinary Reproductive Ultrasonography. Time Mirror International Publishers Limited, London*.PP. 10-81.
- [11] J.F. Pycoc. (2007). Therapy for mares with uterine fluid. In: *Samper, J.C., Pycoc, J.F. and Mackinnon, A.O. (Eds), Current Therapy in Equine Reproduction. Saunders Elsevier, St Louis, CA*, p. 93-104.
- [12] P.L. Sertich, (2007): Pregnancy Evaluation in the Mare. In: *Current therapy in large animal theriogenology. 2nd E.d., Youngquist, R.S. and Threlfall, W.R., Elsevier, Philadelphia, PA, USA*. PP. 99-106.

- [13] M.M. LeBlanc. (2012). Pathogenesis of post-mating induced endometritis and chronic bacterial endometritis. Proceedings of the Annual Meeting of the Italian of Equine Vet. Bolongna, Italy
- [14] H. A. Barbary, I. I. Abo-ghonema, I. E. El-Bawab &M. S. Fadel. (2016). Diagnosis and Treatment of Bacterial Endometritis in Arabian Mares. Alexandria Journal of Veterinary Sciences, 49(2): 116-125.
- [15] J.R. Newcombe (1998): Understanding the cause, significance and treatment of intra-luminal uterine fluid. Journal of Equine Veterinary Science, 18 (2): 74-78.